

Experimental melting of biotite + plagioclase + quartz ± muscovite assemblages and implications for crustal melting

Véronique Gardien,¹ Alan Bruce Thompson, Djordje Grujic, and Peter Ulmer

Department für Erdwissenschaften, ETH Zentrum, Zürich, Switzerland

Abstract. In order to understand the role of mica-rich rocks as a source of granite magmas, a series of melting experiments was performed on two different starting materials. The first composition is a model biotite gneiss consisting of 30 wt % biotite, 30 wt % plagioclase, and 40 wt % quartz. The second composition is a model two-mica pelites consisting of 15 wt % biotite, 15 wt % muscovite, 30 wt % plagioclase, and 40 wt % quartz. Experiments were performed under vapor-absent conditions at 1.0 GPa and between 750° and 950°C. With only biotite in the starting material the volume of melt is always less than 15 vol % below 900°C and reaches 25 vol % at 950°C. In experiments that involve both biotite and muscovite in the starting material, the melt proportion increases up to 28 vol % at 825°C and reaches 60 vol % at 950°C. For the biotite-plagioclase-quartz (BPQ) assemblage, the solidus is located at 800°C at 1.0 GPa. The melting reaction produces a metaluminous granitic liquid and leaves a residuum consisting of garnet + biotite + orthopyroxene + plagioclase + quartz. In addition, the experiments show that at 1.0 GPa biotite can be stable above 950°C. With both micas in the starting material (BPQM), the solidus at 1.0 GPa is located at 750°C. The melting reactions produce a peraluminous granitic liquid and leave a residuum of garnet + sillimanite + biotite + quartz + plagioclase + Kfeldspar in experiments below 900°C. At 950°C the residuum consists of garnet + orthopyroxene + biotite + plagioclase. The melt fraction is determined by the proportions of the hydrous phases and of the amount of feldspar relative to quartz. Mineral modes of the source rocks, particularly the amount of quartz, are at least as important as the amount of available H₂O in controlling the melt fraction generated during crustal anatexis.

Introduction

The quantity of melt generated by anatexis of crustal rocks is determined by the mineral assemblage, the amount of H₂O available, and the temperature attained at a given depth. The melting of common crustal rocks, for example, muscovite-bearing metasediments, amphibolites, and biotite-bearing gneisses that contain H₂O only bound in hydrous minerals, is controlled by vapor-absent melting reactions.

Muscovite-bearing metasediments begin vapor-absent melting near 725°C at 1.0 GPa (~35 km [Storre, 1972; Huang and Wyllie, 1973]) and generate S-type granite [e.g., Thompson, 1982; England and Thompson, 1984; Patiño-Douce and Johnston, 1991]. Temperatures of up to about 800°–850°C can be achieved in the lower part of continental crust that has undergone thickening by collision with reasonable “geotherms and radiogenic heat production” [England and Thompson, 1984; Thompson and Connolly, this issue].

Hornblende-bearing basaltic amphibolites begin vapor-absent melting at temperatures that exceed 925°C at 1.0 GPa [Rushmer, 1991; Wyllie and Wolf, 1993]. The melting of amphibolite in the absence of external H₂O therefore requires either massive basalt injection into the lower continental crust or

asthenospheric impingement under continental crust following delamination of eclogitic thickened lower crust.

Biotite-bearing gneisses are abundant in exposed lower crustal terrain. Their protoliths may have been graywackes and/or compositionally intermediate metavolcanic and plutonic rocks. Vapor-absent melting of biotite in metapelites begins at higher temperature than that of muscovite [Vielzeuf and Holloway, 1988; LeBreton and Thompson, 1988; Patiño-Douce and Johnston, 1991] but at a lower temperature than that of hornblende in amphibolite [Rushmer, 1991], metavolcanics [Conrad et al., 1988], and granodiorite to tonalite [Naney, 1983; Schmidt, 1993]. Fluid-absent melting of muscovite occurs abruptly by virtually univariant reaction because of the restricted variation in composition of this mineral. By contrast, fluid absent-melting of biotite and hornblende takes place over a relatively broad temperature interval because of the large variation in composition of these phases (due to solid solutions).

Muscovite-bearing metapelites are extremely fertile because they are sensitive to vapor-absent melting in collision thickened lower crust. For example, trace element modeling of Himalayan leucogranites [Harris and Inger, 1992; Inger and Harris, 1993] has shown that they were generated by vapor-absent melting of a muscovite-bearing source and the melting of less than 15% of the source rock was required for their generation.

At the present time, the relationships between melt fraction, mineral mode, and temperature are poorly constrained. Generally, it is expected that the amount of muscovite and biotite

¹Now at Laboratoire des Sciences de la Terre, Ecole Normale Supérieure de Lyon, Lyon, France.

Copyright 1995 by the American Geophysical Union.

Paper number 95JB00916.
0148-0227/95/95JB-00916\$05.00

Table 1a. Volume Percent of Minerals of the Starting Materials and the Minerals in the Experiment Products From the Experiments at 1.0 GPa With No Added H₂O

	Bio	Plg	Als	Qtz	Amp	Mus	Gar	Ksp	Liq
VH88	18.8 ^a	17.4 ^a	9.6 ^a	45 ^a		9.4 ^a			
875°C		4.5 ^b	5.5 ^b	10.5 ^b		0 ^b	26.2 ^b		53 ^b
900°C		0 ^b	6.5 ^b	12.9 ^b			22.9 ^b		58 ^b
PdJ 91	26.3 ^a	3.59 ^a	19.8 ^a	34.9 ^a		10.2 ^a	5 ^a		
825°C	27.9 ^b	0 ^b	23 ^b	29 ^b		0 ^b	5.56 ^b		16 ^b
850°C	21 ^b		24 ^b	26 ^b			11.5 ^b		19 ^b
875°C	18.8 ^b		21.4 ^b	20.8 ^b			14 ^b		25 ^b
900°C	16 ^b		20 ^b	13.9 ^b			17.3 ^b		32 ^b
950°C	7 ^b		21.6 ^b	10.3 ^b			21.8 ^b		39 ^b
SJ 92	19.6 ^a	48.4 ^a		30.1 ^a	1.9 ^a				
875°C	19.8 ^b	40.2 ^b		38.2 ^b	3 ^b				2 ^b
900°C	16.3 ^b	40.2 ^b		36 ^b	2 ^b				4.4 ^b
950°C	14.9 ^b	40.2 ^b		33.5 ^b	0 ^b				9.2 ^b
L1, 800°C	27.3 ^a		12.2 ^a	37.2 ^a					6.3 ^b
L2, 800°C	57 ^a	15.3 ^a	8.14 ^a	25 ^a					17 ^b
L3, 800°C	25 ^a	21 ^a	11 ^a	34 ^a			5.13 ^a	3.55 ^a	6.1 ^b

Results are from *Vielzeuf and Holloway* [1988] (VH 88), *Skjerlie and Johnston* [1992] (SJ 92), *Patino-Douce and Johnson* [1991] (PdJ 91), *LeBreton and Thompson* [1988] (L1, L2, L3). Bio, biotite; Plg, plagioclase; Als, aluminum silicate; Qtz, quartz; Amp, amphibole; Mus, muscovite; Gar, garnet; Ksp, K-feldspar; Liq, melt.

in quartz-feldspar assemblages directly governs the amount of anatectic melt at a given temperature [e.g., *Clemens and Vielzeuf*, 1987]. In a previous study involving the melting reaction of biotite + plagioclase + quartz (BPQ I) assemblages [*Gardien et al.*, 1994] we observed that less than 10% melt was formed from 800° to 900°C at 1.0 GPa.

The present study documents the results of experiments undertaken in order to evaluate the effects that the relative proportion of muscovite and biotite, with plagioclase and quartz have on the fraction of melt which can be generated as a function of temperature. The pressure range investigated was that corresponding to the lower parts of thickened continental crust (1.0–2.09 GPa). Because of the difficulties of determining small melt fractions, an image analysis technique using scanning electron microscopy was developed.

Previous Rock-Melting Studies at H₂O Saturation

Numerous studies have shown the importance of the amount of H₂O in the generation of large proportions of melt. Early studies were mostly conducted under H₂O-saturated conditions because of the faster equilibration rates and the belief that granitic magmas were H₂O-saturated. Experiments such as those of *Piwinskii* [1977] on granite, granodiorite, and tonalite have shown that the melt proportion increases rapidly at temperatures higher than the H₂O-saturated solidus. The rapid rise in melt proportion results from the fact that for rocks of granitic and intermediate composition the H₂O-saturated liquidus is only 100°–200°C higher than the H₂O-saturated solidus. Experiments giving rise to large melt fractions are frequently used [e.g., *Bergantz*, 1990] in modeling the ability of the continental crust to generate melt during anatexis, despite the fact that vapor-absent melting reaction is also a viable process for the generation of melt. Because the H₂O solubility of granitic melt increases markedly with pressure, the amount of H₂O required to saturate granitic melt at, for example, 1.0 GPa (≈35 km) is about 18 wt % (60–70 mol %). Such amounts of free H₂O are not expected in the lower continental crust.

Melt Production in Vapor-Absent Melting Experiments

The studies of *Vielzeuf and Holloway* [1988] and *Patino-Douce and Johnston* [1991] on two mica metapelites showed that large proportions of melt (39–58 vol %) are produced between 825° and 900°C. By contrast, for the same pressure and temperature conditions, *LeBreton and Thompson* [1988], *Skjerlie and Johnston* [1993], and our results on BPQ I [*Gardien et al.*, 1994] showed that H₂O-undersaturated melting reactions involving biotite generate small melt proportions (5–15 vol %). As shown in Table 1a, the difference between intermediate rock compositions [*LeBreton and Thompson*, 1988; *Skjerlie and Johnston*, 1993; *Gardien et al.*, 1994] and metapelite [*Vielzeuf and Holloway*, 1988; *Patino-Douce and Johnston*, 1991] is the presence of aluminum silicate and muscovite in the latter. The presence of kyanite cannot be responsible for the production of large proportions of melt because experiments by *LeBreton and Thompson* [1988] have shown that the vapor-absent melting of biotite + kyanite + quartz + plagioclase assemblage generates small proportions of melt (6–15 vol %). Moreover, the greater fertility of the composition used by *Vielzeuf and Holloway* [1988] compared to that of *Patino-Douce and Johnston* [1991] reflects the greater amount of plagioclase in the starting material of the former. In order to understand the role of mica-rich pelites as a source of granitoid magmas, a series of systematic vapor-absent melting experiments was performed on model biotite gneiss (BPQ II) and model two-mica pelites (BPQM) at 1.0 GPa between 750° and 950°C.

The amount of melt produced from vapor-absent melting of muscovite, biotite, and hornblende rock compositions with increasing temperature at 1.0 GPa from various studies is shown in Figure 1. The steeply sloping curve of melt volume percent and shallowly inclined curve of melt volume percent correlate with the melting of specific minerals. The steeply sloping curve characterizes the vapor-absent melting of hydrous minerals which produce a large proportion of melt over a narrow temperature interval as for example muscovite. The shallowly inclined curve reflects the dehydration melting of minerals which

Table 1b. Volumes of Melt Obtained by SEM Image Analysis

	Bio	Plg	Als	Qtz	Amp	Mus	Gar	Ksp	Liq
BPQM	13 ^a	26.8 ^a	0	44.8 ^a		15.3 ^a			
750°	13 ^b		0 ^b			0 ^b	0 ^b		15 ^b
800°									13 ^b
825°	10 ^b	22 ^b	2 ^b	26 ^b			10 ^b		28 ^b
850°									37 ^b
900°	6 ^b	12 ^b	7 ^b				15 ^b		42 ^b
950°	2 ^b	8 ^b	0 ^b	0 ^b			22.5 ^b		>60 ^b
BPQ II	26.8 ^a	28.5 ^a	0 ^a	45 ^a					
750°	26.8 ^b	28.5 ^b	0 ^b	45 ^b					0 ^b
800°									3 ^b
825°	15 ^b	25 ^b		37 ^b			3 ^b		7 ^b
850°									9 ^b
900°	8 ^b	16 ^b		35 ^b			11 ^b		12 ^b
950°									>25 ^b
BPQ I, 10	30 ^a	24 ^a		39 ^a			3 ^b	2 ^a	
800°									1 ^b
850°									2 ^b
875°									5 ^b
900°									6 ^b
BPQ I, 15	30 ^a	24 ^a		39 ^a			3 ^b	1 ^a	
800°									3 ^b
850°									5 ^b
875°									10 ^b
900°									15 ^b

From this study (BPQ II, BPM) and Gardien *et al.* [1994]. Bio, biotite; Plg, plagioclase; Als, aluminium silicate; Qtz, quartz; Amp, amphibole; Mus, muscovite; Gar, garnet; Ksp, K-feldspar; Liq, melt.

^aStarting materials.

^bProducts of experiments.

exhibit extensive solid solution and produce relatively small proportions of melt over a large temperature interval as, for example, biotite and hornblende. An intermediate situation which combines successively steeply sloping and shallowly inclined segments on the melting curve represents the cotectic

melting of the residual assemblage. These results point to the different “fertility” of crustal rocks. Because temperatures in a thickened domain during continental collision rarely exceed about 800°–850°C [e.g., England and Thompson, 1984], vapor-absent melting of many crustal rock types will only generate

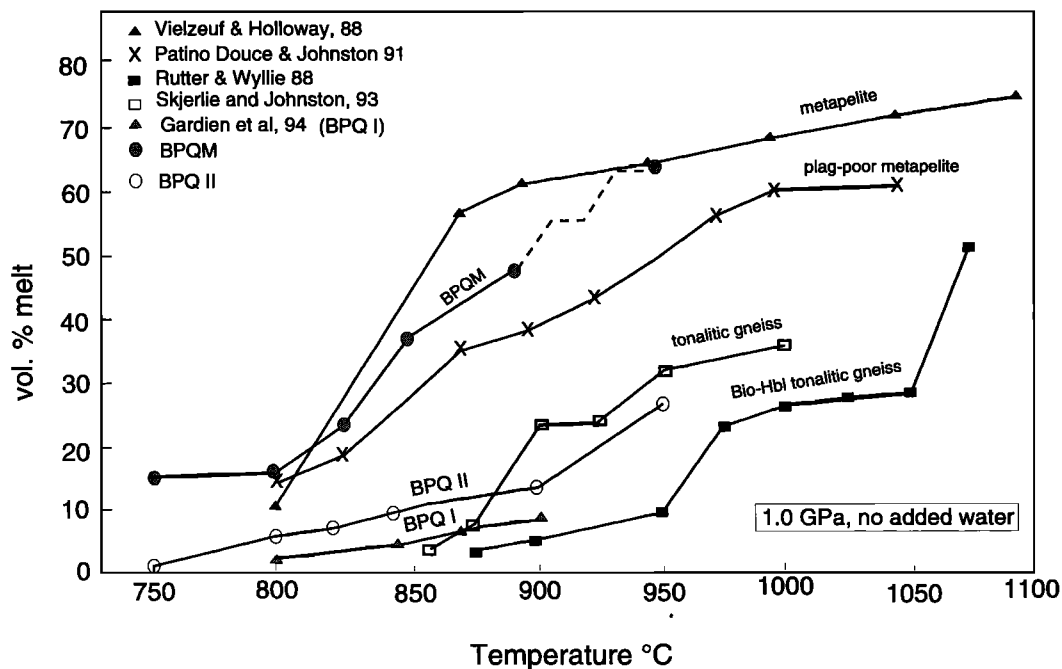


Figure 1. Volume percent of melt versus $T^{\circ}\text{C}$ from vapor-absent experiments of muscovite and biotite in metapelites and graywackes and for amphiboles in tonalites, with increasing temperature at 1.0 GPa and no added water to the system. Such diagrams are useful because they help us to view rock melting in terms of the variables pertinent to the amount of melt expected from various common rock compositions (rock fertility).

Table 2. Characteristics of the Starting Materials

	BPQ I	BPQ II	BPQM	Bio	Mus	Plg
SiO ₂	64.59	68.43	70.04	36.04	44.79	61.06
TiO ₂	0.67	0.81	0.38	2.70	0.16	0
Al ₂ O ₃	16.40	12.45	14.92	17.22	34.02	23.96
FeO total	4.59	6.36	3.65	21.10	3.01	0.12
MnO	0.05	0.12	0.09	0.35	0.16	0.04
MgO	1.37	2.54	1.39	8.46	0.82	0.01
CaO	3.85	1.77	1.79	0.02	0.15	5.89
Na ₂ O	3.58	2.52	2.65	0.09	0.92	8.32
K ₂ O	3.41	3.18	3.18	9.88	9.89	0.73
H ₂ O	1.27	1.82	1.9	3.80	4.17	
Total	100	100	100	99.74	98.39	100.13

	LBT88			VH 88	PdJ 91	SJ 93
	L1	L2	L3			
SiO ₂	62.44	51.57	61.15	64.35	57.36	62.26
TiO ₂	1.07	1.93	0.99	0.82	1.26	0.52
Al ₂ O ₃	19.65	20.18	19.63	18.13	23.24	14.89
FeO total	5.77	10.4	6.84	6.26	8.59	4.67
MnO	0.04	0.05	0.14	0.09	0.17	0.06
MgO	2.58	4.64	2.5	2.44	2.72	1.73
CaO	1.5	0.96	1.45	1.52	0.40	2.93
Na ₂ O	2.33	1.36	2.08	1.66	0.48	4.47
K ₂ O	3.07	5.32	3.18	2.56	3.63	2.05
H ₂ O	1.55	2.63	2.04	2.15		
Total	100	100	100	100	99.54	99.74

In weight percent. BPQ II and BPQM are bulk rock compositions are given with the chemical composition of the minerals. The bulk rock composition of starting materials of Gardien *et al.* [1994] (BPQ I), LeBreton and Thompson [1988] (LBT 88), Vielzeuf and Holloway [1988] (VH 88), Patiño-Douce and Johnston [1991] (PdJ 91), and Skjerlie and Johnston [1992] (SJ 92) are also presented.

small melt proportions. Such small melt fractions (<10 vol %) are difficult to quantify in experimental charges examined only by the optical microscope.

Experimental and Analytical Techniques

Two different mixtures of natural minerals were used as starting materials. The first mixture (BPQ II) combined 30 wt % of biotite + 30 wt % of plagioclase + 40 wt % of quartz (Table 2) and was made in order to have a simple starting material compared with the more complicated composition BPQ I [Gardien *et al.*, 1994] which contained about 6 vol % of accessory minerals (titanite, apatite, and alkali feldspar). In the second mixture (BPQM), 15 wt % of muscovite + 15 wt % of biotite + 30 wt % of plagioclase + 40 wt % of quartz were combined in order to give an average pelitic composition (Table 2). Because the water content in biotite and muscovite is similar (3.8–4.1 wt %, Table 2), the amount of water available from hydrous minerals in the two starting compositions is roughly identical. Any differences between the two sets of results therefore cannot be ascribed to the initial water content of the starting materials. The bulk rock compositions of BPQ and BPQM are presented in Table 2 together with the mineralogical composition of biotite, muscovite, and plagioclase. Bulk rock compositions of the starting materials of LeBreton and Thompson [1988], Vielzeuf and Holloway [1988], Patiño-Douce and Johnston [1991], and Skjerlie and Johnston [1992] are also listed for reference.

All experiments were performed in an end-loaded piston cylinder with 14-mm bore. Fifteen to 20 mg of finely ground starting mixtures were encapsulated in 2.3-mm Ag70-Pd30 containers and welded shut. NaCl and NaCl-Pyrex assemblies

were used as a confining medium. Two capsules containing BPQ II and BPQM mixtures were put simultaneously in the piston cylinder. Pressures were calibrated against the albite-jadeite-quartz equilibrium at 600°C and 1.64 GPa [Johannes *et al.*, 1971], the quartz-coesite transition at 1000°C and 2.97 GPa [Bohlen and Boettcher, 1982], and fayalite-quartz-orthoferrosilite equilibrium at 1000°C and 1.41 GPa [Bohlen *et al.*, 1980]. Pressures are estimated to be precise to within 0.5 kbar of the stated value. Temperatures were measured with Pt-Pt10Rh thermocouples and were controlled to within 2°C. Temperatures were not corrected for the effect of pressure on the emf. Experiment duration varied from 140 to 333 hours.

Because reversal of melting experiments in natural multi-component systems is virtually impossible, attainment of equilibrium cannot be demonstrated rigorously. A number of observations, however, support the assumption that equilibrium was attained: (1) Melt and mineral (biotite, orthopyroxene, and garnet) compositions were found to change regularly throughout the pressure-temperature range investigated. (2) Compositions of melt and minerals were constant throughout any given product of experiment (with the exception of remnant relic cores). (3) Plagioclase, garnet, and orthopyroxene developed euhedral shapes, suggesting that rim analyses are close to equilibrium compositions. Because the experiments were conducted under H₂O-undersaturated conditions, conventional double-capsule oxygen-buffering techniques could not be applied. The f_{O_2} generated by the assembly was estimated to be within the vicinity of the Ni-NiO buffer equilibrium.

Successful experiment products were mounted in epoxy resin and polished to expose the center of the capsule. These

Table 3. Experimental Experiments Conditions and Phase Assemblages for the Experiments at 1.0 GPa

Experiment	T°C	Mix	Time, hours	Phases present
1	750	BPQ II	333	Qtz + Plg + Bio
	...	BPQM		Qtz + Plg + Bio + Ksp + Liq
2	800	BPQ II	270	Qtz + Plg + Bio + Ksp + Liq
	...	BPQM		Qtz + Plg + Bio + Ksp + Liq
3	825	BPQ II	191	Qtz + Plg + Ksp + Bio + Opx + Gar + Liq
	...	BPQM		Qtz + Plg + Ksp + Bio + Sil + Gar + Liq
4	850	BPQ II	145	Qtz + Plg + Ksp + Bio + Gar + Opx + Liq
	...	BPQM		Qtz + Plg + Ksp + Bio + Sil + Gar + Liq
5	900	BPQ II	142	Qtz + Plg + Ksp + Bio + Gar + Opx + Liq
	...	BPQM		Qtz + Plg + Ksp + Bio + Gar + Sil + Liq
6	950	BPQ II	122	Qtz + Plg + Ksp + Bio + Gar + Opx + Liq
	...	BPQM		Plg + Bio + Opx + Gar + Liq

No added H₂O, between 750° and 950°C; modes are presented in Table 1a. Opx, orthopyroxene; Sil, sillimanite.

mounts were subsequently used during scanning electron microscopy (SEM) and electron microprobe analysis. Electron microprobe analysis was performed on a Cameca SX50 using a 15-kV accelerating potential and a 20-nA and 1- μ m focused beam for minerals and a 10-nA and 8- μ m defocused beam for glass. Sodium and potassium were analyzed first in order to minimize the influence of alkali migration under the electron beam. Experimental conditions and the results of the experiments are summarized in Table 3.

Melt Distribution Revealed by SEM Micrographs

The amounts of melt proportion were calculated from back-scattered electron micrographs (BSE) obtained by a JEOL JSM 840 scanning electron microscope (SEM). Calculations of melt fraction were performed by image analysis. The best method is to redraft the BSE images for the specific mineral phase and scan it with a video camera. The images were then analyzed with a commercial program for the Macintosh computer. The recognition of a mineral phase is more precise because it has been previously analyzed with the electron microprobe in order to minimize the subjective factor, i.e., pattern-shape recognition. A range of magnifications was used: large magnification to include the smallest fractions and small magnification to avoid local heterogeneity, and the results were averaged. Compared with the optical microscope, the SEM offers considerably superior resolution up to at least 10,000 times microscope magnification. Moreover, it is possible to detect contrast equivalent to compositional differences of 0.1 Z atomic number [Lloyd, 1987].

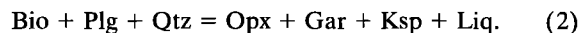
Melting Behavior of the BPQ II Assemblage at 1.0 GPa

The results of the H₂O-undersaturated melting experiments involving the BPQ II starting composition are listed in Table 3. Rutile and alkali feldspar which were not present in the starting material, were observed in the experiment at 750°C. Titanium, alkali feldspar, and H₂O were released from biotite without evidence of melt formation on the BSE micrographs. The absence of melt at 750°C is in agreement with the proportions of phases remaining which are close in proportions to those of the starting material (Table 3). At 800°C the occurrence of rutile and alkali feldspar in the sample is associated

with the formation of small amounts of melt of about 3 vol % (Figure 2a), suggesting the reaction:



The sample at 825°C contained 7 vol % of melt, garnet, orthopyroxene plus quartz, biotite, and plagioclase. Garnet and orthopyroxene grew at the expense of biotite, indicating the exchange reaction:



The location of Opx-in curve has been discussed by *Vielzeuf and Montel* [1994] and located at 860° ± 15°C at 1.0 GPa. Our experiments indicate that the Opx-in curve is located at lower temperature (825°C) and always coincides with the occurrence of garnet and melt. The same assemblage is present at 900°C, where about 12 vol % of melt is observed. The small increase in the melt proportion from 825° to 900°C is associated with an increase in the amount of orthopyroxene, and a decrease in the amount of biotite in the residue (Figure 2b). At 950°C, 25 vol % of melt is observed. Biotite is still present but has decreased and become less aluminous and more titaniferous. The abundance of quartz has decreased, and plagioclase has developed subhedral to euhedral outlines. Figures 2a and 2b are SEM micrographs of BPQ experimental charges at 1.0 GPa and 825° and 900°C respectively. The variations in the proportion of phases for some experiments are listed in Tables 1a and 1b.

Melting Behavior of the BPQM Assemblage at 1.0 GPa

The results of the H₂O-undersaturated melting experiments involving BPQM starting material are presented in Table 3. The samples at 750° and 800°C contain 13–15 vol % melt. Muscovite has completely disappeared, indicating that at 1.0 GPa Mus-out and melt-in curves are located near 750°C, which reduces the wet-solidus temperature by 25°C compared to that of *Storre* [1972]. Sillimanite is not present as a reaction product of muscovite melting, but alkali feldspar is observed. The absence of sillimanite indicates that biotite is capable of incorporating the excess of Al₂O₃ from muscovite (at 750°C the Al₂O₃ content is about 17 wt % in biotite for BPQM and about 13 wt % in biotite for BPQ), while the melt accommodates the potassium (at 750°C the abundance of K₂O in the melt is 2

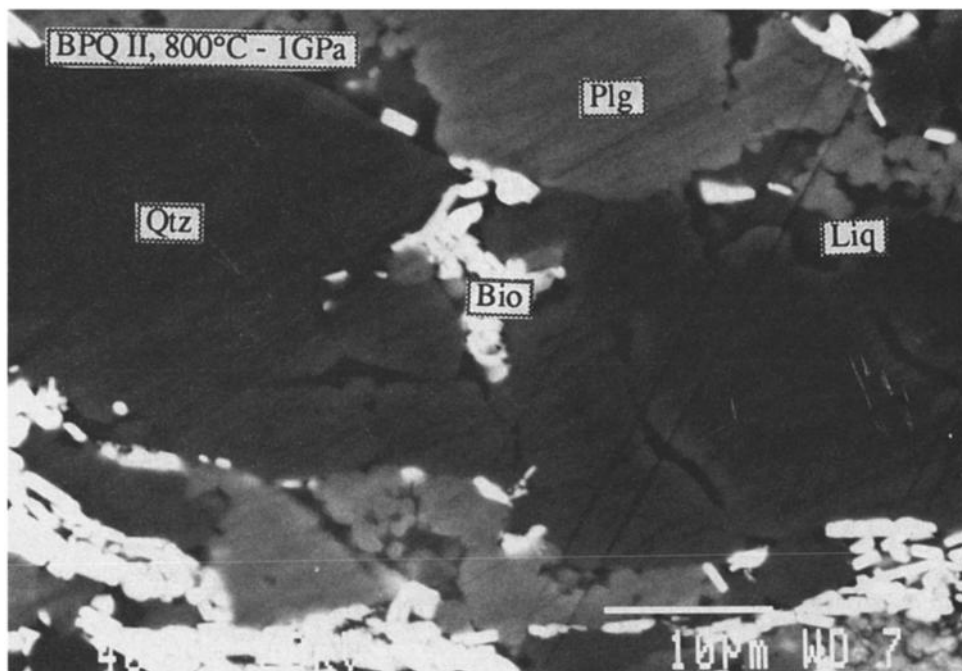


Figure 2a. Backscattered electron image of selected 1.0-GPa experiment products with BPQ II starting material at 800°C. Interstitial melt (Liq) occurs in small pockets between plagioclase (Plg) quartz (Qtz), and biotite (Bio) grains. The rims of melt appear along grain boundaries of quartz/quartz and quartz/plagioclase.

times greater than the abundance of CaO and Na₂O, Table 4). The stability of biotite between 750° and 800°C may explain the absence of garnet in the sample.

At 825°C the sample already contains 28 vol % melt. Sillimanite and garnet grew at the expense of plagioclase and biotite. Figure 3 shows the experimental product held at 1.0

GPa and 825°C. At 900°C, the melt fraction has increased to 42 vol %. Sillimanite associated with garnet is the most abundant phase, whereas the abundance of quartz, plagioclase, and biotite has decreased. The progressive decrease in the amount of alkali feldspar from 825° to 900°C suggests that the latter is a reactant in the reaction:

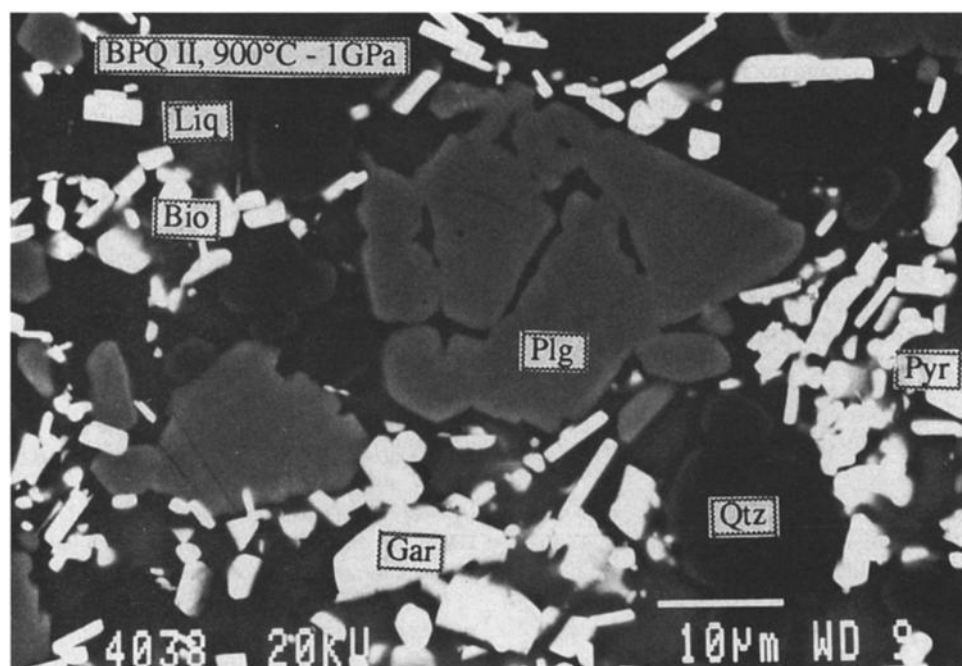
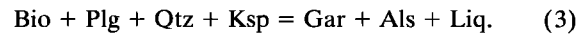


Figure 2b. Backscattered electron image of selected 1.0-GPa experiment products with BPQ II starting material at 900°C. The melt (Liq) is more abundant everywhere in the section surrounding the mineral phases. Newly grown idiomorphic garnet (Gar) and orthopyroxene (Opx) appear to be in equilibrium. Newly formed Al₂O₃ and TiO₂-rich biotite crystals are abundant in the charge.

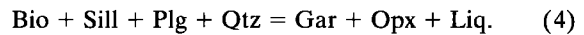
Table 4. Glass Compositions Produced During Experiments With BPQ II and BPQM Starting Mixtures at Various Temperatures and 1.0 GPa

	750 BPQM		825 BPQM		850 BPQM		950 BPQM		825 BPQ		850 BPQ		900 BPQ	
	Example 1	Example 2	Example 1	Example 2	Example 1	Example 2	Example 1	Example 2	Example 1	Example 2	Example 1	Example 2	Example 1	Example 2
	SiO ₂	63.38	63.42	68.45	67.12	66.01	62.76	69.89	69.49	66.50	65.12	66.77	66.96	67.69
TiO ₂	0.05	0.07	0.13	0.12	0.12	0.36	0.36	0.4	0.17	0.32	0.12	0.16	0.17	0.18
Al ₂ O ₃	13.46	13.72	14.99	15.25	14.06	14.54	17.28	19.52	13.27	13.01	13.65	13.58	14.38	14.49
Cr ₂ O ₃	0	0	0	0	0.01	0	0	0	0	0	0	0	0	0
FeO	1.12	0.95	1.39	2.59	1.12	2.58	1.65	1.83	1.60	1.54	1.73	1.16	1.41	1.77
MnO	0.02	0.05	0	0.04	0.02	0.13	0.10	0.03	0.02	0	0	0	0	0.02
MgO	0.07	0.08	0.28	0.34	0.15	0.58	0.39	0.42	1.2	1.44	1.59	1.59	1.97	2.27
CaO	1.28	0.956	2.91	2.18	3.10	1.76	1.04	1.08	2.44	2.87	2.58	2.78	3.95	3.33
Na ₂ O	1.05	2.05	2.52	2.78	2.76	1.87	3.02	2.93	3.01	3.53	3.52	3.56	2.08	2.58
K ₂ O	2.99	2.29	4.89	4.59	4.74	4.81	4.37	4.34	3.58	3.33	4.34	4.72	3.20	3.30
Total	85.43	83.61	93.5	94.01	92.31	93.37	94.89	95.07	91.08	88.19	92.29	91.51	91.05	92.52
Qtz	50.42	47.58	28.66	27.47	26.90	30.03	32.21	35.23	29.47	25.73	22.62	21.64	32.57	29.38
Cor	7.40	7.33	0.29	1.84	0	3.42	5.80	7.08	0.01	0	0	0	0.33	0.65

In weight percent. All the elements were analyzed with 1.0-nA beam currents, 8- μ m defocused, counting time 20 s. Values of ClPW normative quartz (Qtz) and corundum (Cor) are given for each analysis.



At 950°C more than 60 vol % of melt is present in the sample, sillimanite and quartz have disappeared while garnet associated with Al-rich orthopyroxene and plagioclase coexist with the melt. The fact that sillimanite and quartz are no longer present at 950°C indicates the transgression of both Sil-out and Qtz-out curves. The abundance of biotite decreases until only relict patches are present, suggesting that we are close to the Bio-out curve. The disappearance of sillimanite and quartz between 900° and 950°C and the occurrence of orthopyroxene indicate that the following reaction is taking place:



Phase Compositions

Garnet

Garnet is not present either in the starting material or in the products from the experiments conducted at 750°C. From 800° to 950°C, garnet occurs as euhedral unzoned crystal in both the BPQ II and BPQM assemblages. In BPQM, the CaO content of garnet increases from 3 wt % at 825°C to 9.5 wt % at 900°C, whereas both FeO (from 31 to 25 wt %) and MgO (from 3.4 to 2.5 wt %) contents decrease between 825 and 900°C. At 950°C the content of CaO decreases rapidly to 2.8 wt %, while FeO and MgO contents increase to 38 and 7.5 wt %, respectively. The MnO content decreases gradually from 3.4 wt % at 800°C to less than 1 wt % at 950°C. At a given temperature the CaO content is always higher in the BPQM assemblage than in BPQ assemblage. In addition, FeO, MnO, and MgO contents are always lower in the BPQM than in the BPQ II assemblages (Figure 4).

Orthopyroxene

Between 825° and 900°C, orthopyroxene occurs only in the BPQ II products. The most significant change in orthopyroxene composition is the rapid increase in Al₂O₃ content from 2 wt % at 825°C to 7–8 wt % at 900°C, whereas FeO and MgO decrease slightly. At 950°C, orthopyroxene occurs in both the BPQ II and BPQM products with a Al₂O₃ content of 11 wt % (Figure 4), although in neither case is orthopyroxene present with sillimanite.

Plagioclase

CaO and Na₂O contents are virtually constant from 800° to 900°C. In both the BPQ II and BPQM assemblages the plagioclase composition (An_{28–30}) is close to that of the starting material (An₂₇). At 950°C the CaO content increases to An_{35–40}. Despite no alkali feldspar in the starting material it occurs between 800° and 900°C in the BPQ and BPQM assemblages. Potassium content decreases with increasing temperature from Or₈₆ at 800°C to Or₆₃ at 900°C.

Biotite

At 1.0 GPa from 750° to 825°C the composition of biotite does not differ significantly from the biotite of the starting material. The TiO₂ content increases from 2.7 wt % at 825°C to 5 wt % at 950°C in both the BPQ II and BPQM assemblages. An increase in MgO content from 7 wt % at 825°C to 14 wt % at 950°C is coupled with a decrease in FeO content from 20 wt % at 825°C to 12 wt % at 950°C.

The decrease in aluminum content of biotite from BPQ II

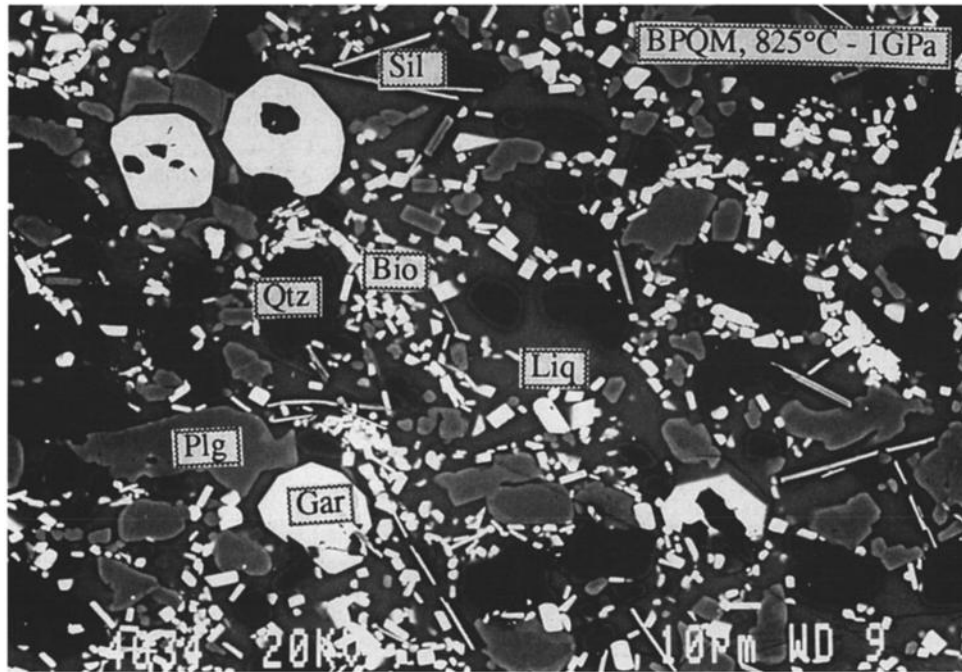


Figure 3. Backscattered electron image of selected 1.0-GPa experiment products with BPQM starting material, at 825°C. Idiomorphic garnet grains (Gar) and needles of sillimanite (Sil), newly formed rims of plagioclase around a core with the starting material composition, and new growth of biotite (Bio) appear to be in equilibrium with the melt (Liq). The stability of garnet, sillimanite, and biotite crystals is demonstrated by the clear contacts of crystals against the melt. Muscovite is not present in this experiment.

and BPQM assemblages could be related to the increase in Al_2O_3 in the melt with increasing temperature (Figure 4). For a given temperature the aluminum content is always highest in BPQM assemblage, whereas FeO and MgO contents are lowest. The TiO_2 content is similar in the two assemblages at any given temperature.

Melt

Microprobe analysis indicate that melts produced during our experiments have a granitic composition (Table 4). With the BPQM assemblage the granitic glass is present in all experimental products from 750° to 950°C. With the BPQ II starting

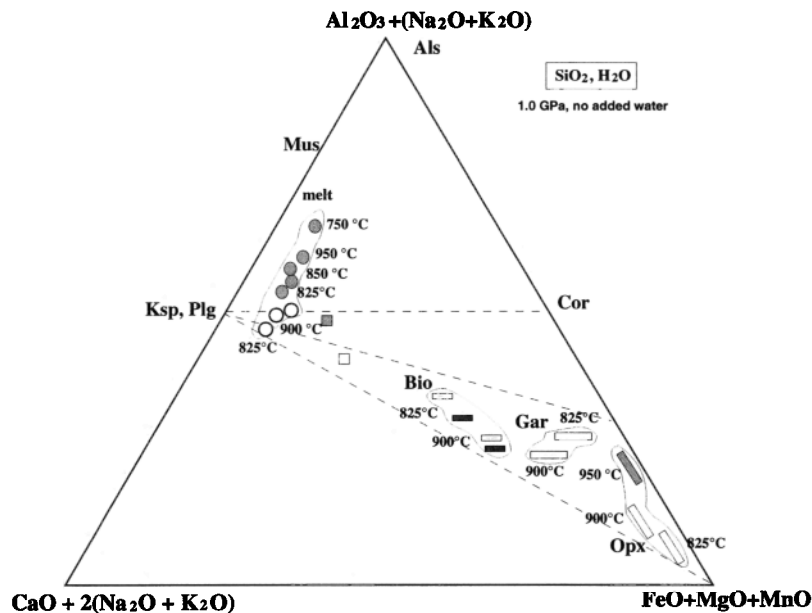


Figure 4. ACF projection (in molar units) showing the starting composition for BPQ II (solid square) and BPQM (open square) and microprobe data for the minerals and glasses at 1.0 GPa, no added water, 750°–950°C. The minerals and glass compositions are shown with open and solid symbols (circles and rectangles) obtained from BPQ II and BPQM, respectively, starting materials.

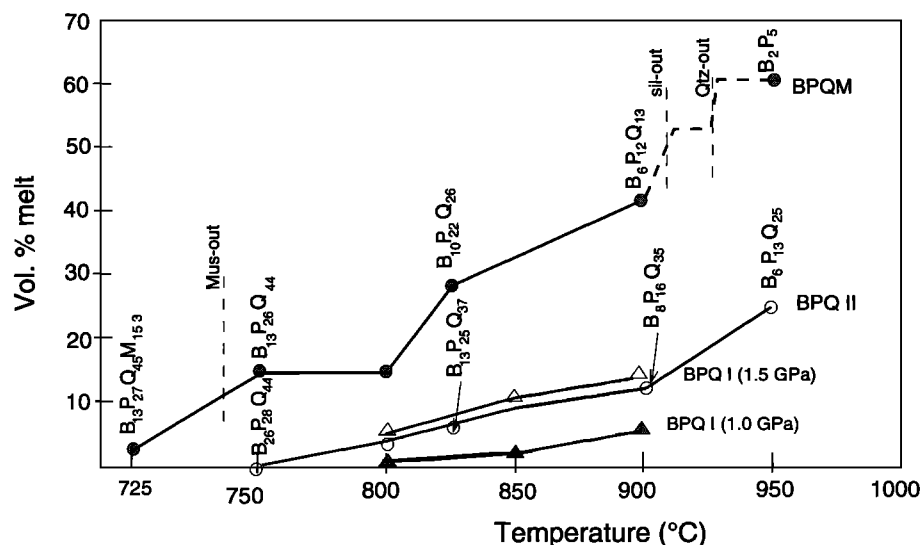


Figure 5. Volume percent of melt versus $T^{\circ}\text{C}$ from vapor-absent melting reaction of muscovite and biotite for metapelites with increasing temperature at 1.0 GPa (BPQM, solid circles, and BPQ II, open circles) and pressure (BPQ I 1.0 GPa, solid triangles, BPQ I 1.5 GPa, open triangles, after Gardien et al. [1994]).

material the melt occurs at 825°C. The heterogeneity in melt composition at low temperatures (750–850°C) reflects the lack of chemical equilibrium between melt pools which are not interconnected. Table 4 and Figure 4 show how the composition of the melt changes as a function of temperature for the BPQ II and BPQM assemblages. With increasing temperature the melt in BPQ II is richer in Al_2O_3 (see the amount of normative corundum in Table 4) and in Na_2O , while FeO, MgO, and K_2O do not differ significantly compared with melts from BPQM experiments. At 750°C and 850°C the enrichment in Al_2O_3 in BPQM compared with BPQ II is related to the disappearance of muscovite in the former. In the BPQM assemblage the significant increase in the amount of Al_2O_3 at 950°C reflects the disappearance of sillimanite as an important aluminous phase.

The first granitic liquid produced with BPQM at 750°C (Table 4) is silica-alumina-, and potassium-rich and contains almost no MgO, FeO, CaO, and Na_2O . The low amounts of MgO, FeO, CaO, and Na_2O in the melt may indicate that plagioclase and biotite do not react at 750°C. The muscovite breakdown produces K-feldspar and a small amount of melt which may contain a lot of H_2O (50% of the initial water available in the starting material). The low total in Table 4 might be a Na volatilization problem (maybe 1 or 2 wt % of Na_2O are missing) due to the very high water content of the melt and also to the difficulty of analyzing very small melt pockets. With increasing temperatures the melt proportion increases with the melting of quartz and plagioclase, but the water content into the melt does not increase because the biotite remains stable until 900°C. The dilution of water increases in the melt with increasing the temperature and explains the high water content in the melt at 750°C and the lowest H_2O content at higher temperatures. The stability of biotite and plagioclase at 1.0 GPa and 750°C is expressed by the volume percent of biotite and plagioclase which are virtually similar (Table 1b) to that of the starting material. The increase in MgO, FeO, CaO and Na_2O in the BPQ II and BPQM glasses over the temperature range of 825–950°C indicates that biotite and plagioclase (+ quartz) react (Table 4).

Figure 5 shows the changes in melt proportion with increasing temperature as indicated in our experiments at 1.0 GPa (BPQ I, BPQ II, and BPQM) and 1.5 GPa (BPQ II). Reaction (3) can be considered as a vapor-absent melting reaction expressed by the steeply sloping curve of melt volume percent at temperatures lower than 750°C for BPQM (Figure 5), whereas the vapor-absent melting reactions (1) and (2) correspond to the shallowly inclined curve of melt volume percent for BPQ I (1.0 and 1.5 GPa) and BPQ II. The cotectic melting of quartz and sillimanite, which is reaction (4), represents the successive steeply sloping and shallowly inclined segments of the melting curve between 900 and 950°C for BPQM. The dashed line indicates that intermediate experiments must be done in order to determine the exact temperature of both the Sil-out and the Qtz-out curves. In general, the melt generated from the BPQ II assemblage is less aluminous (less than 0.65 wt % normative corundum) than that produced from the muscovite-bearing assemblage (between 1 and 7 wt % normative corundum). Silica contents are approximately similar (Table 4). Decomposition of muscovite releases KAlSi_3O_8 and Al_2O_3 which enter the melt and promote the melting of the quartz + plagioclase mixture by lowering its minimum melting temperature. The upper thermal stability of biotite is higher in H_2O -undersaturated than in H_2O -saturated melts [Naney, 1983; Puziewicz and Johannes 1990]. In our BPQM experiments the H_2O released from muscovite increases the amount of water dissolved in the melt, promoting the breakdown of biotite and the rapid increase of the melt fraction up to 28 vol % at 825°C. Moreover, it was observed that for both starting materials the melt becomes more aluminous for temperature increases in agreement with the decrease in alumina content of biotite and the decrease in the amount of biotite with increasing temperature (Table 1b).

Why Is the Melt Fraction Low in BPQ and High in BPQM Melting?

The results of LeBreton and Thompson [1988] at Al_2SiO_5 saturation and Skjerlie and Johnston [1993], as well as the results presented above on BPQ II, show the low amounts of

melt generated at the dehydration melting solidus for biotite. In agreement with the results of *Vielzeuf and Holloway* [1988], *LeBreton and Thompson* [1988] and *Skjerlie et al.* [1993], our experiments show that at 1.0 GPa, biotite breaks down over the temperature interval 825°C to 975°C due to extensive solid solution, just at H₂O saturation [*Hoschek*, 1976].

We suggest that the main difference obtained in melt proportion in experiments by *Skjerlie and Johnston* [1993] and our results (Table 1b) compared with those of *Vielzeuf and Holloway* [1988] and *Patiño-Douce and Johnston* [1991] (Table 1a) reflects the presence of about 10 wt % muscovite in the starting composition of the *Vielzeuf and Holloway* [1988] and *Patiño-Douce and Johnston* [1991] experiments. In our experiments involving BQPM assemblage the vapor-absent melting of muscovite begins at 750°C at 1.0 GPa. Because of restricted solid solution in muscovite compared with biotite, the melting can be viewed as virtually univariant. Breakdown of muscovite releases both H₂O and KAlSi₃O₈ components to the melt, while the Al₂O₃ component is taken up by sillimanite. If the ratio FeO + MgO/Al₂O₃ in the melt is high [*LeBreton and Thompson*, 1988], the Al₂O₃ component is taken up by garnet, cordierite, or spinel depending upon pressure and temperature conditions [*Vielzeuf and Montel*, 1994] or resides in residual phases like biotite (this study) if the ratio is low. The H₂O and alkali feldspar released from vapor-absent melting of muscovite enter the melt and induce large degrees of melt by lowering the melting temperatures of assemblages containing plagioclase and quartz. Moreover, the greater fertility of BPQ II compared with BPQ I [*Gardien et al.*, 1994] reflects the greater amount of plagioclase and quartz in the former (Figure 5) in agreement with the fertility of the composition used by *Vielzeuf and Holloway* [1988] compared with that of *Patiño-Douce and Johnston* [1991]. The proportion of plagioclase and quartz in the starting material is also very important for the generation of melt during anatexis. Thus we suggest that the low melt fraction produced from metaluminous rocks (granodiorite, graywackes, tonalites) is caused by the persistence of biotite until above 950°C, whereas the large melt fraction produced in metapelitic rocks is caused by the near univariant vapor-absent melting reaction of muscovite.

Conclusions

Our experiments have shown that the melting of BPQM and BPQ assemblages begins at 750°C and at 800°C, respectively. Moreover, the vapor-absent melting reaction of two-mica pelites at 1.0 GPa generates a large amount of peraluminous melt (40–60 vol %) between 800° and 900°C with a residuum consisting of garnet, sillimanite, biotite, quartz, and plagioclase. Over the same range of pressure and temperature the vapor-absent melting reaction of biotite gneiss generates only 5–15 vol % of subaluminous to metaluminous melt, and the residuum consists of orthopyroxene, garnet, biotite, plagioclase, and quartz. Muscovite-bearing metapelites are 3–4 times more fertile at any given temperature (Figure 5) at vapor-absent melting than biotite + plagioclase + quartz gneisses over the same temperature interval.

The optimum mineral proportion for generating larger amounts of anatectic melt by vapor-absent melting of hydrous minerals varies with the type of hydrous mineral and the pressure. At the temperature attained in continental collision anatexis (<850°C), metagraywackes and amphibolites generate only small melt fraction. Only muscovite-bearing litholo-

gies will generate large enough melt volumes (>40%) to permit the extraction of the melt from the residual matrix.

The results presented above and other experimental studies suggest a hierarchy of rock fertility to generate melt during anatexis in collision belts. Thus if it can be demonstrated from natural examples that particular magmatic rocks have relatively refractory sources (e.g., metagraywackes or amphibolites), then such source regions must have experienced additional heat input more than that resulting from simple collision processes.

Acknowledgment. Funding for this study was provided by Swiss National Foundation grant 20-36049.92 to R. Schmid.

References

- Bergantz, G. W., Melt fraction diagrams: The link between chemical and transport models, in *Modern Method of Igneous Petrology: Understanding Magmatic Processes*, *Rev. Mineral.*, vol. 24, edited by J. Nicholls and J. K. Russell, pp. 240–257, Mineralogical Society of America, Washington, D. C., 1990.
- Bohlen, S. R., and A. L. Boettcher, The quartz-coesite transformation: A precise determination and the effects of other components, *J. Geophys. Res.*, **87**, 7073–7078, 1982.
- Bohlen, S. R., E. J. Essene, and A. L. Boettcher, Reinvestigation and application of olivine-quartz-orthopyroxene barometry, *Earth Planet. Sci. Lett.*, **47**, 1–10, 1980.
- Clemens, J. D., and D. Vielzeuf, Constraints on melting magma production in the crust, *Earth Planet. Sci. Lett.*, **86**, 287–306, 1987.
- Conrad, W. K., I. A. Nichols, and V. J. Wall, Water saturated and undersaturated melting of metaluminous and peraluminous crustal compositions at 1.0 GPa: Evidence for the origin of silicic magmas in the Taupo Volcanic Zone, New Zealand and other occurrences, *J. Petrol.*, **29**, 765–803, 1988.
- England, P. C., and A. B. Thompson, Pressure-temperature-time paths of regional metamorphism, I, Heat transfer during the evolution of regions of thickened continental crust, *J. Petrol.*, **25**, 894–928, 1984.
- Gardien, V., A. B. Thompson, G. Grujic, and P. Ulmer, The role of the source composition on melt fractions generation during crustal anatexis, *Eos Trans. AGU*, **75**(16) Spring Meeting Suppl., 359, 1994.
- Harris, N. B. W., and S. Inger, Trace element modelling of pelite-derived granites, *Contrib. Mineral. Petrol.*, **11**, 46–56, 1992.
- Hoschek, G., Melting relations of biotite + plagioclase + quartz, *Neues Jahrb. Mineral. Monatsh.*, **2**, 79–83, 1976.
- Huang, W. L., and P. J. Wyllie, Melting relations of muscovite-granites at 35 GPa as a model for fusion of metamorphosed subducted oceanic sediments, *Contrib. Mineral. Petrol.*, **42**, 1–14, 1973.
- Inger, S., and N. Harris, Geochemical constraints on leucogranites magmatism in the Langtang Valley, Nepal Himalaya, *J. Petrol.*, **34**, 345–368, 1993.
- Johannes, W., D. W. Chipman, J. F. Hays, P. M. Bell, H. K. Mao, A. L. Boettcher, R. C. Newton, and F. Seiffert, An interlaboratory comparison of piston cylinder pressure calibration using the albite breakdown reaction, *Contrib. Mineral. Petrol.*, **32**, 24–38, 1971.
- LeBreton, N., and A. B. Thompson, Fluid-absent (dehydration) melting of biotite in metapelites in the early stages of crustal anatexis, *Contrib. Mineral. Petrol.*, **99**, 226–237, 1988.
- Lloyd, G. E., Atomic number and crystallographic contrast images with the SEM: A review of backscattered electron techniques, *Mineral. Mag.*, **51**, 3–19, 1987.
- Naney, M. T., Phase equilibria of rock-forming ferromagnesian silicates in granitic systems, *Am. J. Sci.*, **283**, 93–1033, 1983.
- Patiño-Douce, A. E., and D. Johnston, Phase equilibria and melt productivity in the pelitic system: implications for the origin of peraluminous granitoids and aluminous granulites, *Contrib. Mineral. Petrol.*, **107**, 202–218, 1991.
- Piwinskii, A. J., Experimental studies of igneous rocks series, central Sierra Nevada Batholith, California, Part II, *Neues Jahrb. Mineral. Monatsh.*, 193–215, 1977.
- Puziewicz, J., and W. Johannes, Experimental study of a biotite-bearing granitic systems under water-saturated and water undersaturated conditions, *Contrib. Mineral. Petrol.*, **104**, 397–406, 1990.
- Rushmer, T., Partial melting of two amphibolites: Contrasting results

- under vapor-absent conditions, *Contrib. Mineral. Petrol.*, 107, 41–59, 1991.
- Rutter, J. M., and P. Wyllie, Melting of vapour absent tonalite at 10 kb to simulate dehydration melting in the deep crust, *Nature*, 331, 159–160, 1988.
- Schmidt, M. W., Phase relations and composition in tonalite as a function of pressure: An experimental study at 650°C, *Am. J. Sci.*, 293, 101–160, 1993.
- Skjerlie, K., and A. D. Johnston, Fluid-absent melting behaviour of an F-rich tonalitic gneiss at mid-crustal pressures: Implications for the generation of anorogenic granites, *J. Petrol.*, 34, 785–815, 1993.
- Skjerlie, K., A. E. Patiño-Douce, and A. D. Johnston, Fluid-absent melting of a layered crustal protolith: Implications for the generation of anatectic granites. *Contrib. Mineral. Petrol.*, 114, 365–378, 1993.
- Storre, B., Dry melting of muscovite + quartz in the range $P_S = 7$ GPa to $P_S = 20$ GPa, *Contrib. Mineral. Petrol.*, 37, 87–89, 1972.
- Thompson, A. B., Dehydration melting of pelitic rocks and the generation of H₂O-undersaturated granitic liquids. *Am. J. Sci.*, 282, 1567–1595, 1982.
- Thompson, A. B., and J. A. D. Connolly, Melting of the continental crust: Some thermal and petrological constraints on anatexis in continental collision zones and other tectonic settings, *J. Geophys. Res.*, this issue.
- Vielzeuf, D., and J. Holloway, Experimental determination of the vapor-absent melting relations in the pelitic system, *Contrib. Mineral. Petrol.*, 98, 257–276, 1988.
- Vielzeuf, D., and J. M. Montel, Partial melting of metagreywackes, I, Fluid-absent experiments and phase relationships, *Contrib. Mineral. Petrol.*, 118, 375–394, 1994.
- Wyllie, P. J., and M. B. Wolf, Amphibolites vapor-absent: Sorting out the solidus in Magmatic Processes and Plates Tectonics, edited by H. M. Prichard, *Geol. Soc. Spec. Publ. London*, 76, 405–416, 1993.
-
- V. Gardien, Laboratoire des Sciences de la Terre, Ecole Normale Supérieure de Lyon, 46 Allée d'Italie, 69 344 Lyon Cedex 07, France. (e-mail: vgardien@geologie.ens-lyon.fr)
- D. Grujic, A. B. Thompson, and P. Ulmer, Department für Erdwissenschaften, ETH-Zentrum, CH-8092 Zürich, Switzerland.

(Received August 15, 1994; revised March 1, 1995; accepted March 15, 1995.)